

# Mechanical ion gate for electrospray-ionization ion-mobility spectrometry

Li Zhou · David C. Collins · Edgar D. Lee ·  
Milton L. Lee

Received: 13 June 2006 / Revised: 25 January 2007 / Accepted: 1 February 2007 / Published online: 8 March 2007  
© Springer-Verlag 2007

**Abstract** A novel ion gate for electrospray-ionization atmospheric-pressure ion-mobility spectrometry (ESI-IMS) has been constructed and evaluated. The ion gate consisted of a chopper wheel with two windows—one for periodic ion passage from the ESI source into the drift region and the other for timing and synchronization purposes. The instrument contained a 45.0 cm long drift tube comprising 78 stainless steel rings (0.12 cm thick, 4.90 cm o.d., 2.55 cm i.d.). The rings were connected together in series with 3.34-M $\Omega$  resistors. The interface plate and the back plate were also connected with the first and the last rings, respectively, of the drift tube with 3.34-M $\Omega$  resistors. A potential of  $-20.0$  kV was applied to the back plate and the interface plate was grounded. The drift tube was maintained at an electric field strength of  $\sim 400$  V cm $^{-1}$ . An aperture grid was attached to the last ring in front of a Faraday plate detector, center-to-center. Several sample solutions were electrosprayed at  $+5.0$  kV with  $+500$  V applied to the ion gate. Baseline separations of selected benzodiazepines, antidepressants, and antibiotics were observed with moderate experimental resolution of  $\sim 70$ .

**Keywords** Ion gate · Electrospray ionization · Ion-mobility spectrometry · Resolution

## Introduction

The first successful marriage of electrospray ionization (ESI) with ion-mobility spectrometry (IMS) was reported by Dole and coworkers [1–3]. Using this technique, a liquid sample was directly introduced into the spectrometer, separated, and detected. In the 1980s, Shumate and Hill [4–9] generated ion-mobility spectra of unclustered ions by using a heated drift-gas flow to assist in desolvation. More recently, Dion et al. [10] and Dwivedi et al. [11] reported ESI-IMS detection of nitrates and nitrites of importance to human health and disease. Several groups [12–18] have also used ESI-IMS for analysis of polar organic compounds, for example amino acids, drugs, explosives, and chemical warfare agents (CWAs). Several groups have also shown that polypeptides and proteins can be electrosprayed and their multiply-charged states separated and detected by IMS [4–6, 19–23].

Not only as a detector, ion-mobility spectrometry has come of age as an important separation method by which different compounds can be separated in space after ionization according to their characteristic ion mobilities. Separation times in IMS are typically given in milliseconds. This enables faster analysis than most other conventional separation techniques, for example gas chromatography (GC), liquid chromatography (LC), and capillary electrophoresis (CE). The main limitation of ESI-IMS is, however, its low resolution. This is attributed to several causes. First, a relatively large volume of sample is typically introduced for trace analysis. Solvent evaporation from the electrosprayed fine droplets in the drift region can therefore cause broadening of analyte bands. Second, heat transfer from the atmospheric gas to the sprayed droplets is low, and desolvation cannot be completed effectively before the droplets enter the drift region. Third, the electrical potential

L. Zhou · E. D. Lee · M. L. Lee (✉)  
Department of Chemistry and Biochemistry,  
Brigham Young University,  
Provo, UT 84602-5700, USA  
e-mail: milton\_lee@byu.edu

D. C. Collins  
Department of Chemistry, Brigham Young University-Idaho,  
Rexburg, ID 83460, USA

of the ESI source perturbs the homogeneity of the electric field in the drift region [18, 24, 25].

Another contribution to low resolution in ESI-IMS is unwanted ion penetration through the ion gate [26, 27]. If a Bradbury–Nielsen design [26] is used, percentage levels of electrosprayed ions can drift through the ion gate under the influence of the electric field, even when the ion gate is closed. Ion penetration results in both elevated background and band broadening, which compromise both sensitivity and resolution. To reduce the amount of ion penetration, the orthogonal electric field of the “closed” Bradbury–Nielsen gate must be increased [27].

In this paper, we report a newly designed mechanical “chopper” ion gate that effectively gates sprayed ions from the ESI tip into the drift region of the ion-mobility spectrometer and improves resolution. Applying a voltage to the ion gate and using a high-flow drift gas helped to further improve the performance of ESI-IMS.

## Experimental

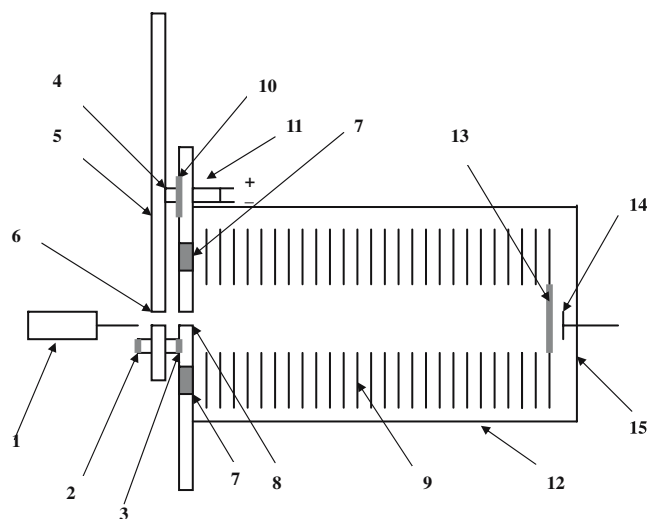
### Materials and chemicals

HPLC-grade methanol and water were purchased from Mallinckrodt Baker (Paris, KY, USA). Glacial acetic acid was obtained from EM Science (Gibbstown, NJ, USA). Benzodiazepines (i.e. diazepam and prazepam), antidepressants (i.e. nortriptyline and imipramine), antibiotics (i.e. ampicillin and cloxacillin), and gramicidin S were acquired from Sigma (St Louis, MO, USA). All solutions were prepared by dissolving the solid analyte compounds in 49.5:49.5:1.0 or 69.5:29.5:1.0 (v/v) methanol–water–acetic acid. Compressed nitrogen (purity 99.9% to 99.99%) was purchased from Airgas (Salt Lake City, UT, USA) and used as drift gas to assist in desolvation and to keep the drift tube free from air contaminants (e.g. water).

### Instrumentation

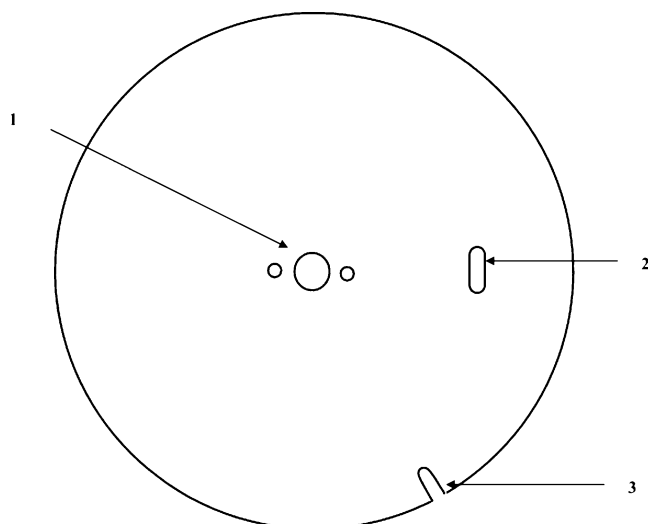
A schematic diagram of the new ESI-IMS system is shown in Fig. 1. The  $\mu$ ESI ion source was operated with a continuous infusion flow rate of 1.0 to 4.0  $\mu\text{L min}^{-1}$  using a syringe pump (Model 55-2222, Harvard Apparatus, Holliston, MA, USA) and a 250- $\mu\text{L}$  syringe with a 21-gauge needle (Gastight; Hamilton, Reno, NV, USA). Tapered fused-silica electrospray tips (~2.5 cm long, 90  $\mu\text{m}$  o.d., 20  $\mu\text{m}$  i.d.) were obtained from Leco (Part 711-955, St Joseph, MI, USA). A potential of +5.0 kV was applied to the  $\mu$ ESI capillary using a high-voltage power supply (Series 230; Bertan, Hicksville, NY, USA).

Figure 2 shows a diagram of the chopper wheel used in the ESI-IMS system. The chopper wheel (3.5 mm thick,



**Fig. 1** Schematic diagram of the ESI-IMS instrument. (1) microspray ( $\mu$ ESI) capillary, (2) optical sensor emitter, (3) optical sensor collector, (4) aluminium adaptor, (5) chopper wheel, (6) inlet window, (7) heating bands, (8) interface plate sampling inlet, (9) drift tube, (10) Teflon washer, (11) DC motor, (12) housing, (13) aperture grid, (14) Faraday plate, (15) back plate

19.2 cm o.d.), similar to that reported by Katta et al. (employing thermospray instead of ESI) [28], was machined from aluminium and electronically insulated from the interface plate by use of a Teflon washer. It contained two oval windows, one as the sensor window (2.0 mm wide, 7.0 mm high) at the edge of the chopper wheel and the other as the sample-inlet window (8.0 mm wide, 3.0 mm high) positioned between the connection holes and the edge of the chopper wheel. By using a separate Bertan Series 230 high-voltage power supply, a potential of +500 V was applied to the rotating chopper wheel with a wire brush to help draw electrosprayed ions into the drift region. A +12 V DC motor (Miniature series; Pittman,



**Fig. 2** Schematic diagram of the chopper wheel. (1) connection holes, (2) sample-inlet window, (3) sensor window

Harleysville, PA, USA) was mounted on and electronically insulated from the interface plate. The chopper wheel was connected with the motor through an aluminium adapter. Using a low-voltage power supply (Model 2762; Heath, Taiwan, ROC), the DC motor rotated the chopper wheel parallel to the interface plate.

For most of the analysis time the ion gate was closed, because the chopper wheel blocked ion transmission from the ESI source into the drift region and also blocked transmission of IR light from the optical sensor emitter (EE-SV3; Omron Electronic Components, Schaumburg, IL, USA) to the collector synchronously. When the sample-inlet window swept across the sampling inlet of the spectrometer, sample from the ESI tip entered the drift region (i.e. the ion gate was open). The distances between the ESI tip and sample-inlet window, and between the sample-inlet window and sampling inlet were 2.0 mm and 5.0 mm, respectively. At the same time, the sensor window swept across the window of the optical sensor. The light signal from the emitter passed through the window to the collector and was detected by the optical sensor. Periodic pulses (pulse rate 5–200 Hz, pulse width 200–500  $\mu$ s) could be generated for initiation and synchronization by simply adjusting the speed of the rotating chopper wheel. In our experiments, for every 100 to 200 ms the chopper ion gate stayed open for 200 to

500  $\mu$ s to enable electrosprayed ions to enter the drift region. The pulse width could also be adjusted without affecting the period by reducing the area of the sample-inlet window with copper tape (Stewart-MacDonald, Athens, OH, USA).

The drift region was operated under atmospheric-pressure conditions ( $\sim$ 650 Torr in Provo, UT, USA). The total length of the drift tube was 45.0 cm. It consisted of 78 stainless steel rings (0.12 cm thick, 4.90 cm o.d., 2.55 cm i.d.). Each stainless steel ring was welded to a 1.0 cm long stainless steel lead. To each lead was attached a high-voltage resistor (3.34 M $\Omega$ , Yageo, Taiwan, ROC). All of the stainless steel rings were separated 4.6 mm apart by ceramic washers (AW Series, Du-Co, Saxonburg, PA, USA) and connected together in series with a high-voltage resistor between each. The first ring of the drift tube was connected to the electrically grounded interface plate with a high-voltage resistor. Two rectangular heating bands (Flexible Series, Watlow, St Louis, MO, USA) were used to heat the interface plate to 50  $^{\circ}$ C and assist in the desolvation of the electrosprayed ions. The temperature in the drift region was 20.0  $^{\circ}$ C and the moisture content in the drift region was  $\sim$ 3 ppm<sub>v</sub>. The round interface plate sampling inlet (2.5 mm i.d.) was centered on the interface plate. The back plate was electrically connected to a high-voltage power supply (Series 225; Bertan) operated at  $-20.0$  kV with a high-voltage

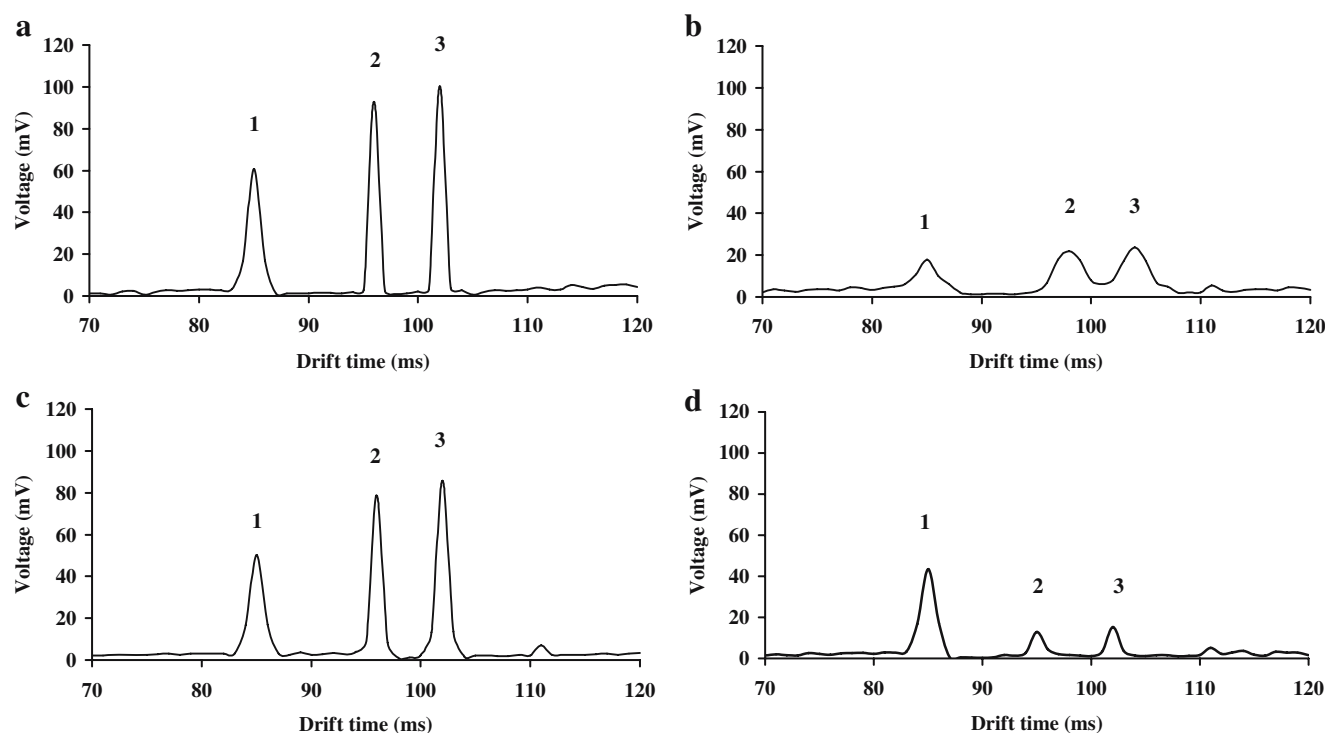


**Fig. 3** Ion-mobility spectra of diazepam (200  $\mu$ mol L $^{-1}$ ) and prazepam (220  $\mu$ mol L $^{-1}$ ) at different gas flow rates with and without potential applied to the ion gate. Conditions: 45.0 cm drift tube, 20.0 kV drift voltage, +5.0 kV electrospray, 20.0  $^{\circ}$ C, 650 Torr, 3.0  $\mu$ L min $^{-1}$  infusion flow rate (methanol–water–acetic acid, 49.5:49.5:1.0, v/v), 64 averages, 0.5 ms gate pulse width. (a) N $_2$  drift gas at 1500 mL min $^{-1}$  and +500 V

applied to the ion gate, (b) N $_2$  drift gas at 100 mL min $^{-1}$  and +500 V applied to the ion gate, (c) N $_2$  drift gas at 900 mL min $^{-1}$  and +500 V applied to the ion gate, (d) N $_2$  drift gas at 1500 mL min $^{-1}$  and “floating” ion gate. Peak identification: (1) solvent, (2) diazepam, (3) prazepam

resistor between the back plate and the last ring of the drift tube. The drift tube was maintained at an electric field strength of  $\sim 400 \text{ V cm}^{-1}$  with a good linear relationship between the ion velocity and electric field strength [1–3]. The current through the drift tube was  $\sim 70 \text{ }\mu\text{A}$ . Nitrogen was used as the drift gas and was introduced into the drift region from two 2.8-mm i.d. holes drilled in the back plate on each side of a mounted, and electrically isolated, Faraday plate detector. The drift gas was adjusted to a flow rate of 100 to  $1500 \text{ mL min}^{-1}$  using a flow meter obtained from Jaco (Berea, OH, USA).

The detector was a small round copper Faraday plate (5.5 mm o.d.) positioned at the end, and in the center of, the drift tube. Attached to the last ring was a stainless-steel screen operated as an aperture grid in the center with the Faraday plate. The aperture grid consisted of parallel stainless steel wires (150  $\mu\text{m}$  o.d.) placed 500  $\mu\text{m}$  apart. Using the aperture grid, induced current, which was generated within the Faraday plate before the ions struck the plate, could be effectively eliminated, thus, reducing peak fronting and improving resolution [27]. When ions struck the Faraday plate a very weak ion current was generated. Using a newly designed in-house current amplifier capable of operating at  $-20.0 \text{ kV}$ , the ion current was amplified (amplification factor  $10^9 \text{ V A}^{-1}$ ), optically transferred, converted to a voltage signal, and finally displayed and recorded using an oscilloscope (9410, Dual 150 MHz; LeCroy, Chestnut Ridge, NY, USA). Data were averaged during acquisition. Depending on the abundance of the analyte ions, 8 to 256 spectra were averaged. Ten determinations of each measurement were made for statistical reason.

#### Safety considerations

Because high voltages were used for the ESI-IMS, safety precautions were taken to protect researchers from electric shock. The high-voltage power supplies and ESI source were electrically shielded using insulated plastic boxes, and moved as far as possible from any metal parts. High-voltage cables were tested for electrical leakage at 1.2 times the highest operating voltage (up to  $+7.0 \text{ kV}$ ) [29].

## Results and discussion

The new ESI-IMS instrument was evaluated and optimized. Measured reduced ion mobility values ( $K_0$ ) were comparable with those reported elsewhere [15, 30–33]. Figure 3a–c show ion-mobility spectra obtained for diazepam ( $200 \text{ }\mu\text{mol L}^{-1}$ ) and prazepam ( $220 \text{ }\mu\text{mol L}^{-1}$ ) at different drift-gas flow rates. At a high flow rate of  $1500 \text{ mL min}^{-1}$  separation of these two compounds was significantly better than at low flow rates of  $100 \text{ mL min}^{-1}$  and  $900 \text{ mL min}^{-1}$  (Table 1).

**Table 1** Comparison of peak-to-peak resolution of diazepam and prazepam in ion-mobility spectra for different drift-gas flow rates

Drift-gas flow rate ( $\text{mL min}^{-1}$ )	Drift time (ms)		$\alpha$	$R_{\text{pp}}$	%RSD
	Diazepam	Prazepam			
1500	95.7	102	1.08	2.88	$\pm 14\%$
900	96.1	103	1.07	1.26	$\pm 15\%$
100	98.1	104	1.06	0.67	$\pm 16\%$

One explanation is that at high flow rates both peaks shifted to faster drift times because of improved declustering. Diazepam moved more than prazepam so these two peaks, which overlapped at  $100 \text{ mL min}^{-1}$ , were completely separated at  $1500 \text{ mL min}^{-1}$ . Adjustment of the selectivity by tuning the drift-gas flow rate was consistent with an earlier report [14]. Figure 3d shows the ion-mobility spectrum obtained for diazepam ( $200 \text{ }\mu\text{mol L}^{-1}$ ) and prazepam ( $220 \text{ }\mu\text{mol L}^{-1}$ ) at a drift-gas flow rate of  $1500 \text{ mL min}^{-1}$  without voltage application to the chopper wheel. Comparison with Fig. 3a shows that applying a potential to the chopper wheel seemed to help draw ions through the sample-inlet window into the drift region of the spectrometer when the ion gate was open. We observed that when a potential of  $+500 \text{ V}$  was applied to the chopper wheel the ion-peak intensities were stronger than without voltage application (Table 2).

Under optimum conditions, a variety of compounds ranging from small molecules to macromolecules were dissolved in buffer solution and analyzed by ESI-IMS. Figure 4 shows an ion-mobility spectrum of a mixture of histidine ( $150 \text{ }\mu\text{mol L}^{-1}$ ), diazepam ( $200 \text{ }\mu\text{mol L}^{-1}$ ), prazepam ( $220 \text{ }\mu\text{mol L}^{-1}$ ), and gramicidine S ( $100 \text{ }\mu\text{mol L}^{-1}$ ) and Fig. 5 shows an ion-mobility spectrum of a mixture of nordoxepine ( $100 \text{ }\mu\text{mol L}^{-1}$ ), imprimine ( $100 \text{ }\mu\text{mol L}^{-1}$ ), ampicillin ( $120 \text{ }\mu\text{mol L}^{-1}$ ) and cloxacillin ( $120 \text{ }\mu\text{mol L}^{-1}$ ). In both spectra baseline resolution is observed for all analyte ions. Multiple peaks (i.e. dimers, trimers, multiply-charged peaks, etc.) could sometimes be observed for single compounds in the ion-mobility spectra. In Fig. 5, the two

**Table 2** Improvements in signal-to-noise ratios and detected ion numbers by applying a potential to the chopper wheel

	Diazepam		Prazepam	
	With potential	Without potential	With potential	Without potential
S/N	130	18.3	140	22.1
$10^5$ Ions/spectrum <sup>a</sup>	6.50	0.89	6.63	1.00
$10^6$ Ions/second <sup>a</sup>	4.31	0.59	4.41	0.70
%RSD	$\pm 11\%$	$\pm 12\%$	$\pm 9\%$	$\pm 13\%$

<sup>a</sup> All ions were assumed to be singly charged

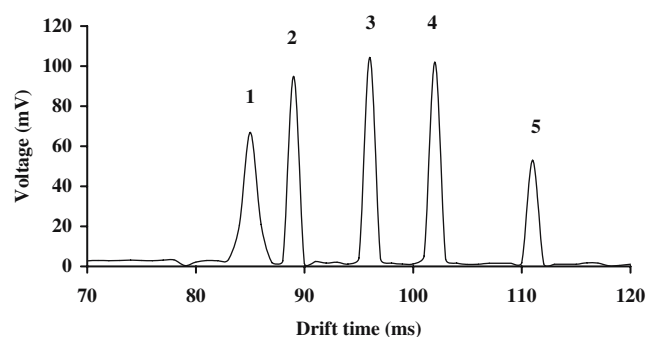


**Fig. 4** Ion-mobility spectrum of a test mixture. Conditions: 45.0 cm drift tube, 20.0 kV drift voltage, +5.0 kV electrospray, 20.0 °C, 650 Torr, 3.0  $\mu\text{L min}^{-1}$  infusion flow rate (methanol–water–acetic acid, 49.5:49.5:1.0, v/v), 64 averages, 0.5 ms gate pulse width,  $\text{N}_2$  drift gas at 1500  $\text{mL min}^{-1}$  and +500 V applied to the ion gate. Peak identification: (1) solvent, (2) histidine (150  $\mu\text{mol L}^{-1}$ ), (3) diazepam (200  $\mu\text{mol L}^{-1}$ ), (4) prazepam (220  $\mu\text{mol L}^{-1}$ ), (5) gramicidin s (100  $\mu\text{mol L}^{-1}$ )

small peaks adjacent to nordoxepine and imprimine are probably ion clusters related to these two compounds. When samples of the two compounds at different concentrations were analyzed, the two small peaks always appeared at approximately the same intensities relative to nordoxepine and imprimine (data not shown). By heating the interface plate and using a long drift tube and low electrospray flow rate, desolvation was usually quite successful and the occurrence of multiple peaks was minimized.

The separation performance of ESI-IMS can be quantified by use of either peak-to-peak resolution or experimental resolution [27]. Peak-to-peak resolution,  $R_{\text{pp}}$ , is defined similarly to that used in chromatography [34]:

$$R_{\text{pp}} = \frac{\sqrt{N}}{4} \left( \frac{\alpha - 1}{\alpha} \right) \quad (1)$$

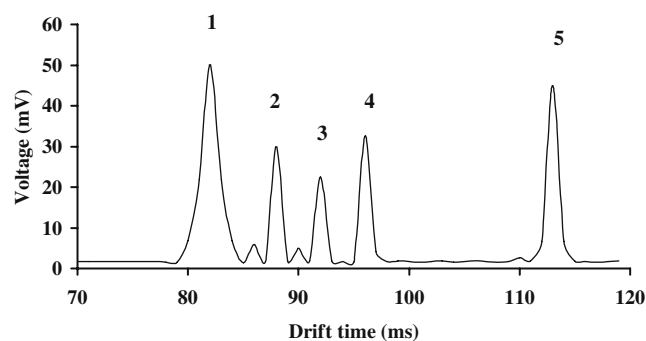


**Fig. 5** Ion-mobility spectrum of a mixture of antibiotics. Conditions: 45.0 cm drift tube, 20.0 kV drift voltage, +5.0 kV electrospray, 20.0 °C, 650 Torr, 3.0  $\mu\text{L min}^{-1}$  infusion flow rate (methanol–water–acetic acid, 49.5:49.5:1.0, v/v), 64 averages, 0.5 ms gate pulse width,  $\text{N}_2$  drift gas at 1500  $\text{mL min}^{-1}$  and +500 V applied to the ion gate. Peak identification: (1) solvent, (2) nordoxepine (100  $\mu\text{mol L}^{-1}$ ), (3) imprimine (100  $\mu\text{mol L}^{-1}$ ), (4) ampicillin (120  $\mu\text{mol L}^{-1}$ ), (5) cloxacillin (120  $\mu\text{mol L}^{-1}$ )

**Table 3** Experimental resolution values determined from ion-mobility spectra of two mixtures

Compound	Drift time (ms)	FWHH (ms)	$R_{\text{e}}^{\text{a}}$
Solvent (Fig. 4)	85.1	1.50	56.7
Histidine	88.9	1.26	70.6
Diazepam	96.2	1.31	73.6
Prazepam	102	1.38	74.1
Gramicidin s	111	1.22	91.1
Solvent (Fig. 5)	82.4	1.50	54.9
Nordoxepine	87.8	1.11	79.1
Imprimine	92.1	1.17	78.7
Ampicillin	95.7	1.20	79.8
Cloxacillin	113	1.30	86.8

<sup>a</sup> %RSD =  $\pm 12\%$

where  $N$  is the plate number and  $\alpha$  is the separation factor. The experimental resolution,  $R_{\text{e}}$ , can be defined as

$$R_{\text{e}} = \frac{t_{\text{d}}}{\omega_{\text{h}}} \quad (2)$$

where  $t_{\text{d}}$  is the drift time and  $\omega_{\text{h}}$  is the full-width-at-half-height (FWHH) of the ion peak.

An obvious difference between  $R_{\text{e}}$  and  $R_{\text{pp}}$  is that only one peak is required to calculate  $R_{\text{e}}$ , whereas two are required to calculate  $R_{\text{pp}}$ . Using the new ESI-IMS instrument,  $R_{\text{e}}$  was calculated to be 55–90, with plate numbers of 120,000–160,000 (Table 3, Figs. 3a, 4, and 5).  $R_{\text{e}}$  was related to the variable desolvating behavior of charged fine droplets and ion clusters. Effective desolvation gave narrow peaks; therefore, different  $R_{\text{e}}$  values were obtained. For prazepam (70  $\mu\text{mol L}^{-1}$ ; Fig. 6) the experimental resolution was 73.6 (%RSD =  $\pm 12\%$ ). Compared with other reports of IMS experimental resolution [14, 30, 35, 36], this value is moderately high.

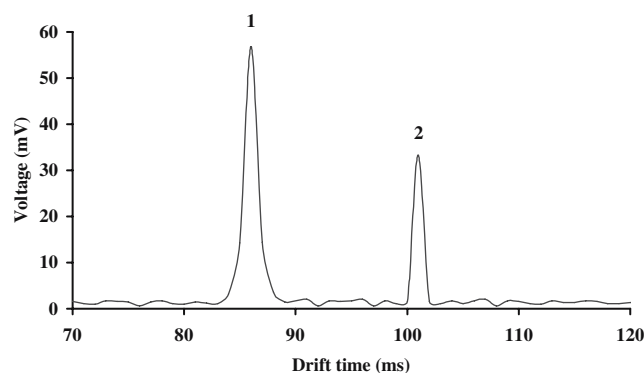


**Fig. 6** Ion-mobility spectrum showing moderate experimental resolution for prazepam (70  $\mu\text{mol L}^{-1}$ ). Conditions: 45.0 cm drift tube, 20.0 kV drift voltage, +5.0 kV electrospray, 20.0 °C, 650 Torr, 2.0  $\mu\text{L min}^{-1}$  infusion flow rate (methanol–water–acetic acid 69.5:29.5:1.0, v/v), 64 averages, 0.5 ms gate pulse width,  $\text{N}_2$  drift gas at 1500  $\text{mL min}^{-1}$  and +500 V applied to the ion gate. Peak identification: (1) solvent, (2) prazepam



## Conclusions

A novel ion gate for IMS has been designed and tested under atmospheric pressure. The ion gate effectively gated electrosprayed ions from the ESI source into the drift region of the IMS system. Both application of a potential to the chopper wheel and use of a high drift-gas flow further improved the performance of the new ESI-IMS system. Baseline separations were observed for mixtures of compounds with moderate experimental resolution of  $\sim 70$ .

**Acknowledgements** We are grateful to Randall W. Waite, Jeffrey L. Jones, and Gary B. Collins (Palmar Technologies, USA) for designing and constructing the detector.

## References

1. Gieniec J, Cox HL, Teer D, Dole M (1972) 20th Annual Conference on MS and Allied Topics, Dallas, TX, pp 276–280
2. Dole M, Gupta CV, Mack LL, Nakamae K (1977) *Polym Prep* 18 (2):188–193
3. Gieniec J, Mack L, Nakamae K, Gupta C, Kumar V, Dole M (1984) *Biomed Mass Spectrom* 11:259–268
4. Shumate CB, Hill HH (1987) 42nd Northwest Regional Meeting of American Chemical Society, Bellingham, WA
5. Shumate CB (1989) Ph.D. Dissertation, Washington State University
6. Shumate CB, Hill HH (1989) *Anal Chem* 61:601–606
7. St. Louis RH, Hill HH (1990) *CRC Crit Rev Anal Chem* 21:321–355
8. McMinn DG, Kinzer JA, Shumate CB, Siems WF, Hill HH (1990) *J Microcol Sep* 2:188–192
9. Hill HH, Siems WF, St. Louis RH, McMinn DG (1990) *Anal Chem* 62:1201A–1209A
10. Dion HM, Ackerman LK, Hill HH (2002) *Talanta* 57:1161–1171
11. Dwivedi P, Matz LM, Atkinson DA, Hill HH (2004) *Analyst* 129:139–144
12. Lee D, Wu C, Hill HH (1998) *J Chromatogr A* 822:1–9
13. Asbury GR, Wu C, Siems WF, Hill HH (2000) *Anal Chim Acta* 404:273–283
14. Collins DC, Lee ML (2001) *Fresenius J Anal Chem* 369:225–233
15. Beegle LW, Kanik I, Matz LM, Hill HH (2001) *Anal Chem* 73:3028–3034
16. Steiner WE, Clowers BH, Matz LM, Siems WF, Hill HH (2002) *Anal Chem* 74:4343–4352
17. Matz LM, Hill HH (2004) *Anal Chem* 74:420–427
18. Tam M, Hill HH (2004) *Anal Chem* 76:2741–2747
19. Smith RD, Loo JA, Ogorzalek RR, Busman M, Udseth HR (1991) *Mass Spectrom Rev* 10:359–452
20. Wittmer D, Chen YH, Luckenbill BK, Hill HH (1994) *Anal Chem* 66:2348–2355
21. Chen YH, Hill HH (1994) *J Microcol Sep* 6:515–524
22. Clowers BH, Hill HH (2005) *Anal Chem* 77:5877–5885
23. Liu Y, Valentine SJ, Conterman AE, Hoaglund CS, Clemmer DE (1997) *Anal Chem* 69:728A–735A
24. Shumate CB (1994) *Trends Anal Chem* 13:104–109
25. Siems WF, Wu C, Tarver EE, Hill HH, Larsen PR, McMinn DG (1994) *Anal Chem* 66:4195–4201
26. Bradbury NE, Nielsen RA (1936) *Phys Rev* 49:388–393
27. Spangler GE (2002) *Intl J Mass Spectrom* 220:399–418
28. Katta V, Rockwood AL, Vestal ML (1991) *Intl J Mass Spectrom Ion Process* 103:129–148
29. Kramer H (1998) *Part Sci Technol* 16:69–76
30. Wu C, Siems WF, Asbury GR, Hill HH (1998) *Anal Chem* 70:4929–4938
31. Johnson PV, Kim HI, Beegle LW, Kanik I (2004) *J Phys Chem A* 108:5785–5792
32. Matz LM, Hill HH, Beegle LW, Kanik I (2002) *J Am Soc Mass Spectrom* 13:300–307
33. Guevremont R, Siu KWM, Wang J, Ding L (1997) *Anal Chem* 69:3959–3965
34. Asbury GR, Hill HH (2000) *J Microcol Sep* 9:172–178
35. Wu C, Siems WF, Hill HH (2000) *Anal Chem* 72:391–395
36. Wu C, Siems WF, Klasmeier J, Hill HH (2000) *Anal Chem* 72:396–403